Ignition and Extinction of Flames Near Surfaces: Combustion of CH_4 in Air

D. G. Vlachos, L. D. Schmidt, and R. Aris
Dept. of Chemical Engineering and Materials Science and Army High Performance Computing Research Center, University of Minnesota, Minneapolis, MN 55455

Ignition and extinction characteristics of homogeneous combustion of methane in air near inert surfaces are studied by numerical bifurcation theory for premixed methane/air gases impinging on planar surfaces with detailed chemistry involving 46 reversible reactions and 16 species. One-parameter bifurcation diagrams as functions of surface temperature and two-parameter bifurcation diagrams as functions of equivalence ratio and strain rate are constructed for both isothermal and adiabatic walls. Lean and rich composition limits for ignition and extinction, and energy production are determined from two parameter bifurcation diagrams. For a strain rate of 500 s^{-1}, CH_4/air mixtures exhibit hysteresis from ~0.5% up to ~12.5% and from ~5.5% up to ~13.5% near isothermal surfaces and adiabatic walls, respectively. Ignition temperature rises with composition from 1,700 to 1,950 K, without a maximum around the stoichiometric ratio. Under some conditions multiple ignitions and extinctions can occur with up to five multiple solutions, and wall quenching, kinetic limitations, and transport can strongly affect flame stability. Flames near the stoichiometric ratio cannot be extinguished by room temperature surfaces for sufficiently low strain rates. The role of intermediates in enhancing or retarding ignition and extinction is studied, and implications of the effect of catalytic surfaces on homogeneous ignition and extinction are discussed. Removal of H atoms and CH_3 radicals by wall adsorption can increase extinction and ignition temperature of 6% CH_4 in air by up to 300 K for a strain rate of 500 s^{-1}.

Introduction

Ignition and extinction of exothermic reactions near walls have many important applications. They define the regime of multiplicity and instabilities of chemical reactors and provide information about stability and safety issues. Methane is the major constituent of natural gas, and CH_3 radical reactions can be very important in the combustion and pyrolysis of larger hydrocarbons (Warnatz, 1984). Thus, understanding of ignition and extinction of CH_4 near surfaces and the role of intermediates on them is crucial if combustion processes are to be used efficiently and safely.

Extensive research has been done on homogeneous combustion of CH_4. Most recent studies using detailed chemical kinetic mechanisms have examined the role of strain rate on the extinction of counterflow jets, either symmetric or asymmetric configurations, for example, Rogg (1988) and Giovangigli and Smooke (1987), in order to simulate the interaction between flamelets encountered in turbulent combustion.

The role of walls on ignition and extinction of premixed mixtures is poorly understood. To our knowledge the only theoretical studies of homogeneous ignition of combustible gases impinging on surfaces use global one step kinetics (Law, 1978; Song et al., 1991b; Smith et al., 1971; Alkidas and Durbetaki, 1971) or asymptotic approximations (Law, 1978; Law and Chung, 1983). The lack of detailed calculations of ignition are primarily due to computational problems near ignition when elementary kinetics are used in the governing equations. In addition, most experiments on ignition refer to

Correspondence concerning this article should be addressed to L. D. Schmidt.
Current address of D. G. Vlachos: Dept. of Chemical Engineering, University of Massachusetts, Amherst, MA 01003.

stationary gases and not to the ignition problem in the stagnation region of a hot surface, for example, Sharma and Sirignano (1969), Laurendeau (1982), and Lewis and von Elbe (1987). However, in many practical applications the velocity of flowing gases can strongly affect flame ignition and extinction.

Homogeneous combustion is affected by surfaces, as compared to freely propagating flames, through momentum, energy, and mass coupling. Thermal coupling between inert surfaces and the homogeneous phase has been thought to play the most important role. Sufficiently hot walls or particles can ignite the homogeneous phase, and this is important in hot wires and foils used as ignitors and in safety (ignitions and explosions) (Bond, 1991). On the other hand, sufficiently cold walls can extinguish flames, and this can be undesired in reactor operation since it leads to reactor instabilities, low conversion and heat production, emission of unburned hydrocarbons or in devices such as flame traps. Accurate calculation of extinction points is essential in heat exchange applications because heated material can cool hot walls and also extinguish flames.

In addition to thermal coupling, chemical coupling between surfaces and the gas phase can also be significant. If surfaces exhibit catalytic activity (as happens with most solids, especially at sufficiently high temperatures), intermediate species can be common to both gas and surface reaction paths, and reaction coupling can then be crucial. Catalysts can also deplete the reactants in the boundary layer, and this effect has been thought to explain the increase of homogeneous combustion ignition temperature in the presence of catalysts (Coward and Guest, 1927; Coward and Greenwald, 1928; Laurendeau, 1982; Griffin and Pfefferle, 1990; Lewis and von Elbe, 1987). Inert surfaces provide valuable information about materials with low catalytic activity such as quartz.

We have recently examined ignition and extinction of H_2/air mixtures near isothermal, constant power, and adiabatic inert walls for flow impinging on a flat plate (Vlachos et al., 1993). We found unexpected bifurcation behavior with up to five solutions for certain conditions. Here, we study ignition and extinction of CH_4 in air near isothermal walls as functions of equivalence ratio and flow rate. Combustion of CH_4/air mixtures near constant power and adiabatic walls will also be discussed briefly. The selectivities and compositions as functions of surface temperature, equivalence ratio, and strain rate will be discussed in the second part of this article.

Model and Numerical Methods

The model considered here is the stagnation point flow geometry of laminar premixed gases impinging on a flat surface. This geometry exhibits many advantages such as spatial and chemical uniformity (desired in chemical vapor deposition of thin films) and large heat-transfer coefficients used in cooling of microelectronics circuits and possibly for energy production from combustible mixtures (Kee et al., 1993). Aside from the practical applications of this flow, it is also very appealing for modeling because it allows a transformation of the two-dimensional equations into one-dimensional, two point boundary value problem.

The partial differential equations, the appropriate boundary conditions, and the transformation for the stagnation point flow are described in detail elsewhere (Sharma and Sirignano, 1969; Vlachos et al., 1993). The dimensionless equations for axisymmetric flow are:

$$\frac{d^3f}{d\eta^3}+f\frac{d^2f}{d\eta^2}+\frac{1}{2}\left(\frac{\rho_o}{\rho}-\left(\frac{df}{d\eta}\right)^2\right)=0, \tag{1}$$

$$\frac{d^2T}{d\eta^2}+f\cdot Pr\frac{dT}{d\eta}+\frac{Pr}{2\alpha\rho c_p}\sum_{i=1}^{n_g}(-\Delta H_i r_i)=0, \tag{2}$$

$$\frac{d^2W_j}{d\eta^2}+f\cdot Sc_j\frac{dW_j}{d\eta}+\frac{Sc_jM_jR_j}{2\alpha\rho}=0, \quad j=1,\ldots,m_g, \tag{3}$$

$$R_j=\sum_{i=1}^{n_g}(\nu_{ij}r_i), \tag{4}$$

where f is the stream function, η is the dimensionless distance, ρ is the gas density, c_p is the specific heat of the mixture at constant pressure, T is the temperature, Pr is the Prandtl number, W_j, Y_j, and M_j are the mass fraction, mole fraction, and molecular weight of species j respectively, Sc_j is the Schmidt number of species j, $-\Delta H_i$ and r_i are the heat of reaction and reaction rate of the ith reaction respectively, R_j is the rate of formation or consumption of species j, ν_{ij} is the stoichiometric coefficient of species j in reaction i, α is the strain rate (velocity gradient), n_g is the number of gas-phase reactions, and m_g is the number of gas-phase species (not counting N_2). Hereafter the subscripts o and s denote ambient and surface, respectively.

In Eqs. 2 and 3, it is assumed that the Schmidt number of all species and the Prandtl number are constant throughout the flame and are calculated at ambient conditions. Giovangigli and Smooke (1987) found that the Lewis number changes by 2-3% throughout the CH_4/air flame. For relatively dilute mixtures, which are mainly studied here, the species flux is approximated by Fick's first Law, and the diffusivity of each species is calculated in N_2 because N_2 is in abundance.

The system of Eqs. 1-4 is complemented by boundary conditions. The ambient composition and temperature are specified, and the velocity far from the surface is assumed to be described by potential flow (Dixon-Lewis et al., 1984). At the surface ($\eta=0$ in transformed domain, $z=0$ in physical domain), no slip or penetration of the fluid occur, the species flux is taken to be zero (for inert surfaces), and the surface temperature is an independent (bifurcation) variable.

The differential equations and boundary conditions are discretized to a set of algebraic equations using second-order finite difference. Central finite difference is employed in the interior of the computational domain whereas three point forward or backward finite difference is used at the ends of the computational domain of length $\eta=6$ (z_o in physical domain). Calculation of flame structures is performed using arc-length continuation. The solution method employed here is quite different than either fully unsteady-state simulations (where integration in time is performed to reach the steady state) (Spalding and Stephenson, 1971; Rogg, 1989) or a hybrid method which switches between a steady-state procedure where Newton's method is used (with insertion of grid points) to time dependent integration (whenever Newton's method fails to converge) (Grcar et al., 1986; Rogg, 1989; Miller et al., 1990).

Details of the simulations are given elsewhere (Vlachos et al., 1993).

An alternative formulation for stagnation flow with a finite length scale has been discussed by Kee and coworkers (Kee et al., 1988), and has been shown to result in different structure and extinction characteristics of flames. The numerical bifurcation applied here is suitable for this flow transformation as well. Since ignition is kinetically limited, it is not expected that use of the alternative formulation would result in strong changes of ignition temperatures. However, extinction temperatures can be different than those calculated here.

The chemistry of the C1 path for combustion of CH_4 is taken from Giovangigli and Smooke (1987) and listed in Table 1. The C2 path, that is, conversion of CH_4 to higher hydrocarbons, is not considered here because mostly fuel lean mixtures are examined (to complete the bifurcation behavior we also have examined fuel rich mixtures). It is known that the C2 path, which involves about two hundred reactions (Westbrook and Dryer, 1984), becomes important for sufficiently fuel rich mixtures. Thus, it is expected that the bifurcation diagrams shown below are slightly inaccurate for these mixtures. Study of the role of C2 path on the bifurcation behavior of fuel rich mixtures is in progress.

All reactions are considered to be reversible. The reaction rate constants of the reverse reactions and the transport properties are calculated using the CHEMKIN thermodynamic and transport database respectively (Kee et al., 1990, 1991). The reaction rate constant of the forward reaction is $k = k_o T^{\beta} \exp(-E/RT)$, where k_o is the preexponential, β is the temperature exponent, and E is the activation energy (in Table 1 $\bar{\omega}$ is the third body efficiency). Analysis of data is performed by plotting one-parameter bifurcation diagrams (response curves), two-parameter bifurcation diagrams (parameter vs. parameter curves), and profiles of temperature and species at different values of the independent variables. Calculation of a Z-shaped curve such as that shown in Figure 1a requires about 25 min CPU time on the Cray X-MP-EA of the Minnesota Supercomputer Institute and many hours are needed to compute a two parameter bifurcation diagram such as that shown in Figure 3c.

Table 1. CH_4-Air Reaction Mechanism (Units in mol, cm^3, K, and cal/mol)

Reaction	k_o	β	E
(1) $CH_4 + M \rightleftharpoons CH_3 + H + M$	0.100E+18	0.000	86,000
(2) $CH_4 + O_2 \rightleftharpoons CH_3 + HO_2$	0.790E+14	0.000	56,000
(3) $CH_4 + H \rightleftharpoons CH_3 + H_2$	0.220E+05	3.000	8,750
(4) $CH_4 + O \rightleftharpoons CH_3 + OH$	0.160E+07	2.360	7,400
(5) $CH_4 + OH \rightleftharpoons CH_3 + H_2O$	0.160E+07	2.100	2,460
(6) $CH_2O + OH \rightleftharpoons H_2O + HCO$	0.753E+13	0.000	167
(7) $CH_2O + H \rightleftharpoons H_2 + HCO$	0.331E+15	0.000	10,500
(8) $CH_2O + M \rightleftharpoons H + HCO + M$	0.331E+17	0.000	81,000
(9) $CH_2O + O \rightleftharpoons OH + HCO$	0.181E+14	0.000	3,082
(10) $HCO + OH \rightleftharpoons H_2O + CO$	0.500E+13	0.000	0
(11) $HCO + M \rightleftharpoons H + CO + M$	0.160E+15	0.000	14,700
(12) $HCO + H \rightleftharpoons H_2 + CO$	0.400E+14	0.000	0
(13) $HCO + O \rightleftharpoons OH + CO$	0.100E+14	0.000	0
(14) $HCO + O_2 \rightleftharpoons HO_2 + CO$	0.300E+13	0.000	0
(15) $CO + O \rightleftharpoons CO_2$	0.320E+14	0.000	−4,200
(16) $CO + OH \rightleftharpoons CO_2 + H$	0.151E+08	1.300	−758
(17) $CO + O_2 \rightleftharpoons CO_2 + O$	0.160E+14	0.000	41,000
(18) $CH_3 + O_2 \rightleftharpoons CH_3O + O$	0.700E+13	0.000	25,652
(19) $CH_3O + M \rightleftharpoons CH_2O + H + M$	0.240E+14	0.000	28,812
(20) $CH_3O + H \rightleftharpoons CH_2O + H_2$	0.200E+14	0.000	0
(21) $CH_3O + OH \rightleftharpoons CH_2O + H_2O$	0.100E+14	0.000	0
(22) $CH_3O + O \rightleftharpoons CH_2O + OH$	0.100E+14	0.000	0
(23) $CH_3O + O_2 \rightleftharpoons CH_2O + HO_2$	0.630E+11	0.000	2,600
(24) $CH_3 + O_2 \rightleftharpoons CH_2O + OH$	0.520E+14	0.000	34,574
(25) $CH_3 + O \rightleftharpoons CH_2O + H$	0.680E+14	0.000	0
(26) $CH_3 + OH \rightleftharpoons CH_2O + H_2$	0.750E+13	0.000	0
(27) $CO + HO_2 \rightleftharpoons CO_2 + OH$	0.580E+14	0.000	22,934
(28) $H_2 + O_2 \rightleftharpoons OH + OH$	0.170E+14	0.000	47,780
(29) $H_2 + OH \rightleftharpoons H_2O + H$	0.117E+10	1.300	3,626
(30) $O_2 + H \rightleftharpoons OH + O$	0.513E+17	−0.816	16,507
(31) $H_2 + O \rightleftharpoons OH + H$	0.180E+11	1.000	8,826
(32) $O_2 + H + M \rightleftharpoons HO_2 + M^*$	0.210E+19	−1.000	0
(33) $O_2 + H + O_2 \rightleftharpoons HO_2 + O_2$	0.670E+20	−1.420	0
(34) $O_2 + H + N_2 \rightleftharpoons HO_2 + N_2$	0.670E+20	−1.420	0
(35) $OH + HO_2 \rightleftharpoons O_2 + H_2O$	0.500E+14	0.000	1,000
(36) $H + HO_2 \rightleftharpoons OH + OH$	0.250E+15	0.000	1,900
(37) $O + HO_2 \rightleftharpoons O_2 + OH$	0.480E+14	0.000	1,000
(38) $OH + OH \rightleftharpoons H_2O + O$	0.600E+09	1.300	0
(39) $H_2 + M \rightleftharpoons H + H + M^{**}$	0.223E+13	0.500	92,600
(40) $O_2 + M \rightleftharpoons O + O + M$	0.185E+12	0.500	95,560
(41) $OH + H + M \rightleftharpoons H_2O + M^{***}$	0.750E+24	−2.600	0
(42) $H + HO_2 \rightleftharpoons H_2 + O_2$	0.250E+14	0.000	700
(43) $HO_2 + HO_2 \rightleftharpoons O_2 + H_2O_2$	0.200E+13	0.000	0
(44) $H_2O_2 + M \rightleftharpoons OH + OH + M$	0.130E+18	0.000	45,500
(45) $H + H_2O_2 \rightleftharpoons H_2 + HO_2$	0.160E+13	0.000	3,800
(46) $OH + H_2O_2 \rightleftharpoons H_2O + HO_2$	0.100E+14	0.000	1,800

* $\bar{\omega}_{32}(H_2O) = 21\bar{\omega}_{32}(Ar)$, $\bar{\omega}_{32}(H_2) = 3.3\bar{\omega}_{32}(Ar)$, $\bar{\omega}_{32}(N_2) = \bar{\omega}_{32}(O_2) = 0$.
** $\bar{\omega}_{39}(H_2O) = 6\bar{\omega}_{39}(Ar)$, $\bar{\omega}_{39}(H) = 2\bar{\omega}_{39}(Ar)$, $\bar{\omega}_{39}(H_2) = 3\bar{\omega}_{39}(Ar)$.
*** $\bar{\omega}_{41}(H_2O) = 20\bar{\omega}_{41}(Ar)$.

Real Variables

In a laboratory experiment, the ambient temperature, the mixture composition, the inlet velocity, and the wall temperature (or the voltage input to the surface) are the control variables. The inlet velocity enters the model through the strain rate (velocity gradient) α. The relationship between the strain rate and the inlet velocity depends on the reactor geometry (Smith et al., 1971; Chin and Tsang, 1978; Annamala and Sibulkin, 1979); for a nozzle of diameter d the velocity v_o is given by:

$$v_o = \alpha \cdot d, \tag{5}$$

that is, the velocity is proportional to the strain rate. In the computations, for each strain rate the axial velocity can be determined at the edge of the boundary layer by (Sharma and Sirignano, 1969; Rogg, 1988)

$$v_o = -\sqrt{2\alpha\nu_o} f_o, \tag{6}$$

where ν_o is the kinematic viscosity at ambient.

The conservation equations are given in dimensionless form in Eqs. 1-3. For stagnation point flow, the distance in the physical domain along the stagnation line can be extracted (Sharma and Sirignano, 1969; Smith et al., 1971), after the solution has been obtained, from an integration according to:

$$z = \int_0^{\eta} \frac{\rho_o}{\rho(\eta')} \sqrt{\nu_o/2\alpha}\, d\eta'. \tag{7}$$

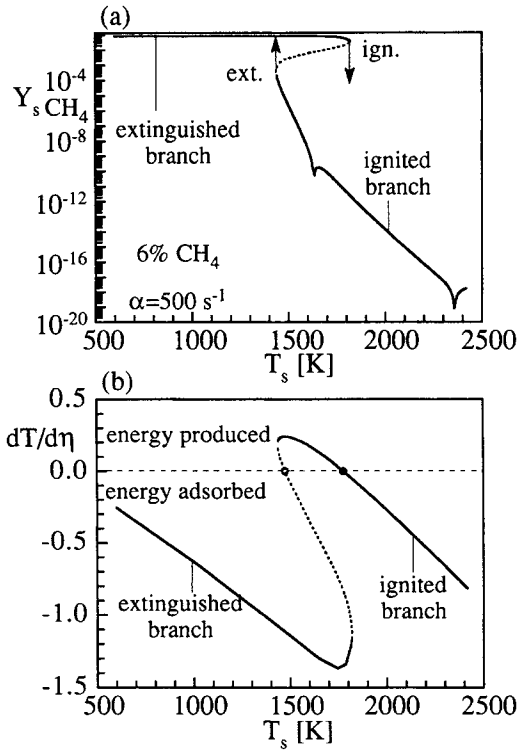

Figure 1. a. Surface mole fraction of CH_4 vs. surface temperature for 6% CH_4 in air with $\alpha = 500\ s^{-1}$; three steady-state states are found for certain surface temperatures. In the absence of Hopf bifurcation the extinguished and ignited branches are stable (solid line) and the intermediate branch is unstable (dotted line). b. Surface temperature gradient $dT/d\eta$ vs. surface temperature.

The two circles indicate van't Hoff points and the dashed line divided the space for energy production and energy removal.

In figures we show position z along the axis of symmetry rather than the dimensionless distance η. For the CH_4 flames shown below, the distance z_o (corresponding to $\eta = 6$) is only a few millimeters, that is, flames considered here are boundary layer flames. Increase of η from 6 to larger values does not affect the solution, that is, potential flows with ambient temperature and mixture composition are usually approached in less than 1 cm.

Role of Wall Temperature

Figure 1 shows results for 6% CH_4 in air vs. the surface temperature T_s for a strain rate of $\alpha = 500\ s^{-1}$. This behavior is typical of mixtures with less than 7.5% CH_4 in air. Upon heating, CH_4 remains very unreactive up to quite high temperature ($T_s \sim 1{,}700$ K), as shown in Figure 1a. This branch of solutions exhibits low reactivity (extinguished branch). Upon further increase in temperature, a turning point (ignition) is found where the slope of the solution with respect to the wall temperature becomes infinite. In a laboratory experiment, when the surface temperature reaches the ignition point ($T_{ig} \sim 1{,}800$ K), the system would jump to the ignited branch indicated by a vertical arrow in Figure 1a. For an electrically heated wall with constant voltage, the increased reaction heat generation would produce a higher temperature on the ignited branch (tilted arrow).

Using the arc-length continuation method, solutions are continued on the unstable branch until another turning point (extinction) is reached. After this point, solutions are continued on the third branch which exhibits substantial combustion (ignited branch). As the surface temperature decreases along the ignited branch towards extinction, CH_4 combustion becomes progressively more incomplete. The CH_4 surface mole fraction Y_{sCH_4} is reduced from $\sim 10^{-16}$ at $\sim 2{,}200$ K to $\sim 10^{-4}$ at $\sim 1{,}500$ K. An extinction would be observed at $T_{ex} \sim 1{,}500$ K where the system would jump to the extinguished branch, as indicated by the second vertical arrow in Figure 1a. Even though the surface mole fraction of CH_4 is relatively low at the cusp shown at $T_s \sim 1{,}600$ K, the cusp is probably a real characteristic of low strain rates and sufficiently rich mixtures.

Figure 1b shows the temperature gradient adjacent to the wall vs. the surface temperature. The two circles indicate points where the temperature gradient at the wall is zero ($dT/d\eta = 0$ at $\eta = 0$). These points are called the van't-Hoff points, and correspond to unstable and stable operation of an adiabatic wall. van't-Hoff points have been used in the past as ignition criterion, for example, Song et al. (1991a). At these two points the system can operate without energy supply in the absence of other energy losses. Along the continuation path and between the two van't-Hoff points the temperature gradient is positive, that is, energy (due to conduction) flows towards the wall whereas in the rest of the arc length the temperature gradient is negative, that is, energy (due to conduction) flows from the surface to the gas phase. Thus, the stable part of the solution within the two van't-Hoff points also determines the conditions for energy production by fuel combustion. As combustion takes place closer to extinction, the temperature gradient (conductive heat flux) increases. However, we find that close to extinction the amount of CH_2O increases slightly (Vlachos et al., 1994). Thus, a tradeoff exists in operation between high energy efficiency, pollutant formation, and reactor stability.

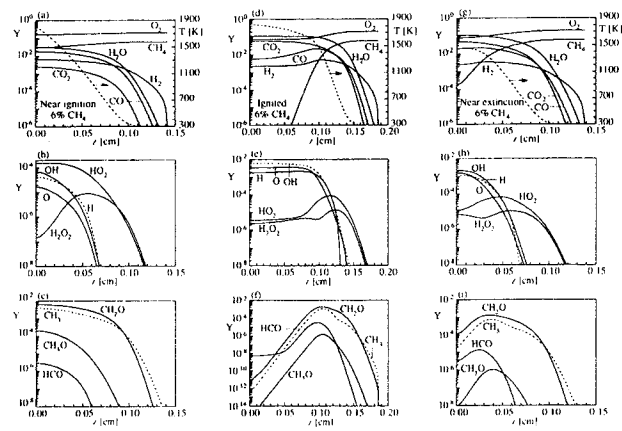

Figure 2. Temperature and species profiles just before ignition ($T_s = T_{ig}$) (a-c), after ignition ($T_s = T_{ig}$) (d-f), and just before extinction ($T_s = T_{ex}$) (g-i), for 6% CH_4 in air with $\alpha = 500\ s^{-1}$.

Upon ignition the flame moves off the wall. As the wall quenches the flame, the flame moves toward the surface.

Profiles of temperature and species just before ignition ($T_s = T_{ig}$ on the extinguished branch), after ignition ($T_s = T_{ig}$ on the ignited branch), and just before extinction ($T_s = T_{ex}$ on the ignited branch) for 6% CH_4 in air are shown in Figure 2. At ignition, the maximum temperature is on the surface, as shown in Figure 2a, and thus energy must be supplied to the system from the hot wall. The mole fractions of CO, CO_2, H_2O, and H_2 change slowly vs. the distance from the wall for ~1 mm and then drop abruptly to zero, as indicated in Figure 2a. H_2O_2 is the only species which exhibits a maximum off the surface, as shown in Figure 2b. While high amounts of H and O atoms and OH radicals are restricted only near the wall where the temperature is high, the mole fraction of HO_2 remains high further away from the wall because reactions R32–R34, which compete with the chain branching reaction R30, are favored at low temperatures. Figures 2a–2c indicate that large fractions of CH_3 radicals and CH_2O are formed near the wall where reaction of CH_4 also occurs.

Upon ignition of the mixture, the flame moves *considerably* off the surface, as shown in Figures 2d–2f. CH_4 reacts completely before it reaches the surface, and the mole fractions of CO, CO_2, H_2, and H_2O change gradually with the distance from the wall until small reactivity of CH_4 is observed. CO_2 is favored over CO near the wall where the temperatures are high, but the opposite is true upstream where the temperature is low, as shown in Figure 2d. High temperature and fractions of H, O, and OH are observed for ~1 mm away from the wall, as shown in Figure 2e. Low temperatures upstream favor the formation of HO_2 radicals at the expense of OH radicals and O atoms. The carbon species shown in Figure 2f peak off the surface where high reactivity of CH_4 occurs.

Figures 2g–2i show profiles of temperature and species at extinction (turning point). Comparison of Figures 2d–2f with 2g–2i indicates that the flame is pushed toward the wall as the surface temperature decreases. Near extinction, combustion of CH_4 occurs close to the surface but does not completely deplete the deficient reactant. Figure 2g shows that the temperature peaks off the surface and conductive heat flows toward the wall. As the temperature decreases along the ignited branch, the regime where the temperature and the fractions of H, O, and OH are high is confined only near the wall. When the pool of H, O, and OH is sufficiently poor, the flame extinguishes.

Role of Equivalence Ratio

Figures 1 and 2 consider in more detail ignition and extinction of fuel lean mixtures (6% CH_4 in air). Figures 3a and 3b show representative response curves (surface mole fraction of CH_4 vs. surface temperature) for fuel lean to stoichiometric and stoichiometric to fuel rich mixtures respectively with a strain rate of $\alpha = 500\ s^{-1}$ and the inset in panel c is a blowup of the five solutions for 12.3% CH_4 in air (the ignited branch is not shown for clarity). The bifurcation behavior is summarized in the two parameter bifurcation diagram Figure 3c which shows the wall temperature at ignition, extinction, and adiabatic operation (triangles) vs. the equivalence ratio ϕ (ratio of fuel to air over fuel to air at stoichiometric for complete oxidation of CH_4 to CO_2 and H_2O. A stoichiometric mixture corresponds to $\phi = 1$, fuel lean mixtures where air is in excess correspond to $\phi < 1$, and fuel rich mixtures where fuel is in

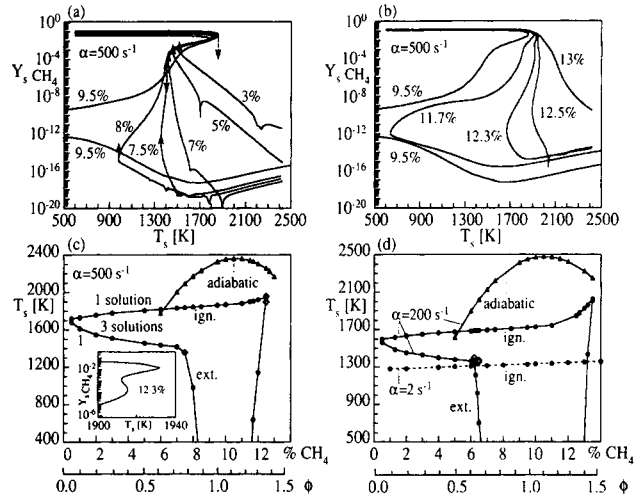

Figure 3. Surface mole fraction of CH_4 vs. surface temperature for selected fuel lean to stoichiometric (a) and stoichiometric to fuel rich mixtures (b) with $\alpha = 500\ s^{-1}$.

Multiple ignitions and extinctions are possible with up to five multiple solutions. Inset (c) shows a blowup of the five solutions for 12.3% CH_4 in air. Two parameter bifurcation diagram (c) for $\alpha = 500\ s^{-1}$ depicts ignition, extinction, and adiabatic operation points vs. ambient composition (equivalence ratio). Solid lines (d) show the corresponding two parameter bifurcation diagram for $\alpha = 200\ s^{-1}$, and the dashed line shows ignition temperatures vs. ϕ for $\sigma = 2\ s^{-1}$. The ignition temperature increases with strain rate.

excess correspond to $\phi > 1$). Figure 3c is constructed by a continuation of the turning points shown in Figures 3a and 3b with the equivalence ratio as the primary bifurcation parameter.

Figure 3c indicates that the homogeneous ignition temperature of CH_4/air mixtures *increases with equivalence ratio* and there is no maximum at the stoichiometric ratio, in agreement with experimental data for CH_4 and natural gas over relatively inert surfaces (Coward and Guest, 1927; Coward and Greenwald, 1928; Laurendeau, 1982; Griffin and Pfefferle, 1990; Lewis and von Elbe, 1987). The extinction temperature decreases slightly with equivalence ratio up to ~7.3%, above which it changes sharply. Richer mixtures cannot be extinguished even by room temperature walls. As the composition rises above ~11.7% CH_4 in air, the extinction temperature rises very sharply. Figure 3c indicates that extinction is more sensitive than ignition to changes of equivalence ratio.

The transition from gradual to abrupt variation of extinction temperatures with equivalence ratio is followed by the appearance of a second set of turning points, examples of which are indicated in Figure 3a for 7.5% and in Figure 3b for 12.3% and 12.5%. For a narrow range of compositions *up to five multiple solutions can coexist*. The extinction point of this second set of saddle node bifurcation points is the one that survives as ϕ increases from low values whereas the extinction point of the first set of saddle mode bifurcation points and the ignition point of the second set annihilate as ϕ increases. These multiplicity phenomena are similar to homogeneous combustion of H_2 in air (Vlachos et al., 1993) whose reaction mechanism is a subset of the CH_4 reaction mechanism.

When $\alpha = 500\ s^{-1}$, hysteresis is observed even for very lean mixtures, as shown Figure 3c. The minimum composition where

the ignition and extinction points coincide (called a cusp point) indicates the minimum equivalence ratio where multiplicity occurs. Very lean mixtures do not generate sufficient radicals and energy to cause ignition of a flame, and thus, at smaller equivalence ratios than that of the cusp point, burning occurs without hysteresis. Another cusp point exists for fuel rich mixtures, as shown in Figure 3c, above which no multiplicity is observed. For mixtures of higher equivalence ratio, burning occurs but without hysteresis. These two cusp points correspond to lean and rich flammability limits for an isothermal surface.

Heated walls extend *both* the lean and rich flammability limits over adiabatic walls. Very lean mixtures can be burned near isothermal heated walls (by providing energy) whereas the minimum composition of CH_4/air mixtures which can be burned near adiabatic walls or using symmetric counterflow jets is ~4-5%, as shown in Figure 3c. Adiabatic walls can sustain a flame at compositions larger than the right cusp point shown in Figure 3c. However, combustion near insulated walls is possible only up to ~13% whereas burning of rich mixtures near heated walls is possible (by providing energy) for even richer mixtures. The limits of adiabatic wall operation, which actually correspond to turning points of an isola, determine the composition range within which energy can be produced.

The bifurcation behavior and flame stability vs. ϕ are compared at different strain rates in Figures 3c and 3d. The solid lines in Figure 3d show homogeneous ignition, extinction, and adiabatic operation points vs. equivalence ratio for $\alpha = 200\ s^{-1}$ and the dashed line shows homogeneous ignition temperatures for $\alpha = 2\ s^{-1}$. At low strain rates there is sufficient time for reaction and formation of reactive intermediates. This behavior has many interesting consequences. The homogeneous ignition temperature increases as the strain rate (flow rate or inlet velocity) increases. At low strain rates the region of compositions which cannot be extinguished by cold walls is wider and adiabatic operation is observed over a wide range of compositions, that is, insulated walls can support leaner and richer mixtures at low flow rates. Furthermore, the cusp point observed for fuel rich mixtures moves to the right (richer mixtures) and the regime of 5 multiple solutions is also wider (compare the diamonds in Figure 3c with the diamonds in Figure 3d). At low strain rates the rich flammability limit calculated based on the C1 reaction path can be considerably high. As an example, we find ignition for $\alpha = 2\ s^{-1}$ up to 20% CH_4 in air (not shown) where the simulation was stopped because the C2 reaction path would dominate the bifurcation behavior.

Figure 4 shows profiles of temperature and species after ignition ($T_s = 1{,}844$ K) for 8%, 9.5%, and 11.7% CH_4/air flames with $\alpha = 500\ s^{-1}$ and indicates the role of equivalence ratio on combustion and flame location. As the composition increases from 6% (Figure 2) to 8% and to 9.5%, the flame moves from ~1 mm to ~2 mm, and to ~3 mm away from the wall. Further increase of the equivalence ratio pushes the flame back toward the wall. Thus, the maximum distance of CH_4/air flames from the wall occurs *around* the stoichiometric ratio. For the stoichiometric mixture the reaction zone is more narrow, as indicated by the profiles of carbon species. As ϕ increases the maximum temperature rises and high temperatures are observed even far from the wall. A double peak in CH_3 profiles is found for 8% and 9.5% CH_4/air mixtures.

Figure 5 shows profiles of temperature and species for low

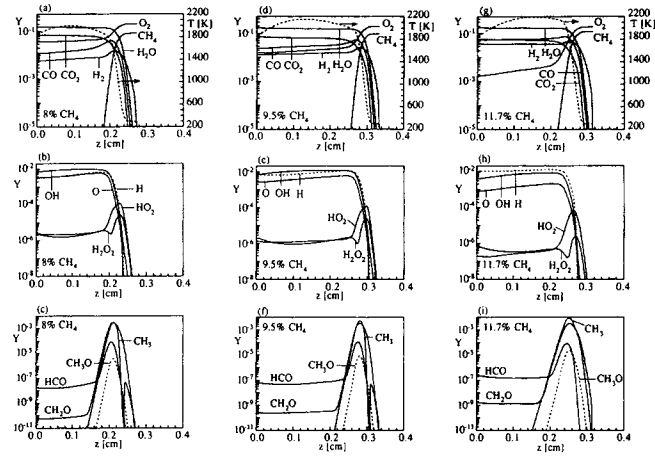

Figure 4. High temperature profiles: temperature and species at $T_s = 1844$ K for 8% (a-c), 9.5% (d-e), and 11.7% (g-i) with $\alpha = 500\ s^{-1}$.

Distance of flames from the wall is maximum for mixtures around the stoichiometric ratio. These flames exhibit high temperatures for relatively long distances away from the wall.

wall temperature for the three mixtures shown in Figure 4. At low surface temperatures, high temperature gradients develop near the surface which is important in energy production. Near the wall HCO, CH_2O, and HO_2 increase considerably. For mixtures around the stoichiometric ratio, wall quenching results in a reduction of H and O atoms and OH radicals but only near the wall, that is, the flame is at sufficiently long distance from the wall that the thermal coupling between the surface and the flame is weak and extinction of flames is impossible by cold walls.

Sensitivity Analysis

The sensitivity of saddle node bifurcation points on kinetic

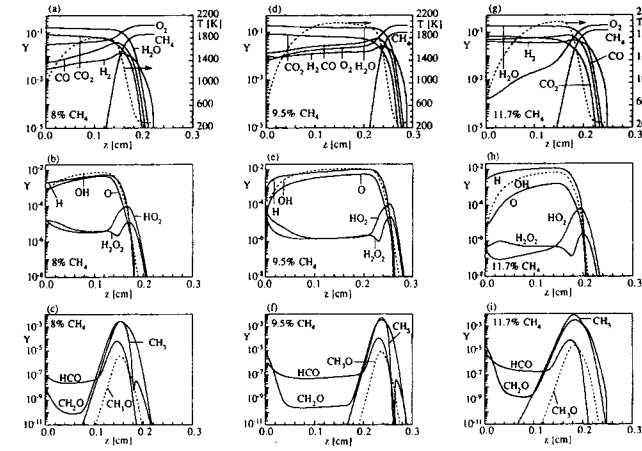

Figure 5. Low temperature profiles of temperature and species for 8% at $T_s = 900$ K (a-c), 9.5% at $T_s = 460$ K (d-e), and 11.7% at $T_s = 640$ K (g-i) with $\alpha = 500\ s^{-1}$.

At low surface temperatures, high temperature gradients can develop near the surface. Mixtures around the stoichiometric ratio can have a weak thermal coupling with the surface.

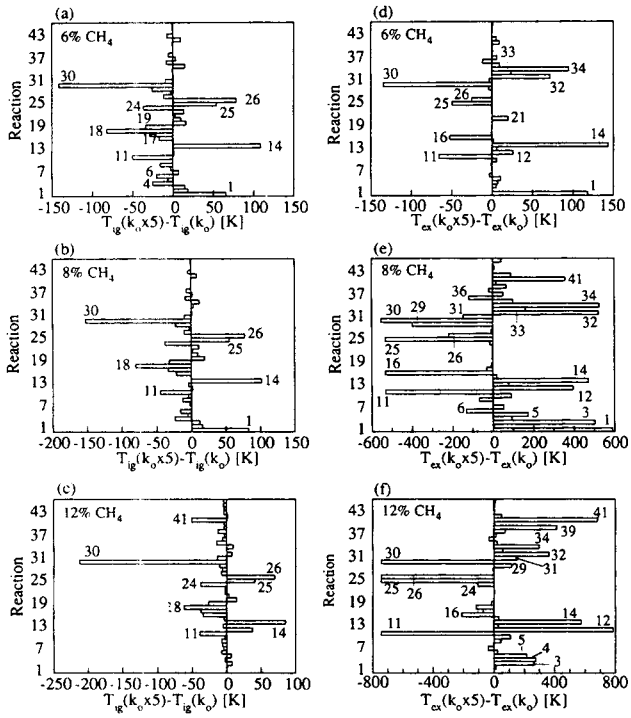

Figure 6. Change shown in ignition temperature of 6% (a), 8% (b), and 12% (c) respectively when the preexponential k_o of the forward reaction is increased by a factor of 5; (d-f) show the corresponding change in extinction temperature with $\alpha = 500\ s^{-1}$.

For 12%, the extinction temperatures for reactions 11, 25, 26 and 30 drop below room temperature (not shown in scale).

data and the importance of reaction steps on ignition and extinction were examined by increasing the preexponential k_o of the forward reaction of each reaction step shown in Table 1 by a factor of 5. The results for two fuel lean (6% and 8%) and one fuel rich (12%) CH_4/air mixtures when $\alpha = 500\ s^{-1}$ are shown in Figure 6.

Figure 6a shows the change in ignition temperature upon increase of k_o for 6% CH_4 in air. Ignition of lean CH_4/air mixtures depends strongly on the following reactions:

$$CH_4 + M \rightleftharpoons CH_3 + H + M \quad \text{(R1)}$$

$$HCO + M \rightleftharpoons H + CO + M \quad \text{(R11)}$$

$$HCO + O_2 \rightleftharpoons HO_2 + CO \quad \text{(R14)}$$

$$CH_3 + O_2 \rightleftharpoons CH_3O + O \quad \text{(R18)}$$

$$CH_3 + O \rightleftharpoons CH_2O + H \quad \text{(R25)}$$

$$CH_3 + OH \rightleftharpoons CH_2O + H_2 \quad \text{(R26)}$$

$$O_2 + H \rightleftharpoons OH + O \quad \text{(R30)}$$

The thermal decomposition of CH_4 (reaction R1) is an endothermic reaction which is favored only at high temperatures. At low temperatures, CH_3 radicals formed by the attack of CH_4 by OH, O, and H recombine with H atoms to form CH_4 reducing H atoms (very active centers) and increasing the ignition temperature. Reaction R11 converts HCO radicals into H atoms which further attack CH_4 and O_2 and results in reduction of the ignition temperature. Reaction R14 has a major retarding effect on ignition. It produces HO_2 which consumes H atoms (reaction R42) and consumes/produces O and OH (reactions R27, R35, R36, R37). Reaction R18, a chain branching reaction, converts molecular oxygen into atomic oxygen which is more reactive in attacking CH_4 and leads to reduction of ignition temperature. Reactions R25 and R26 (a termination reaction) reduce the concentrations of O and OH respectively and increase the ignition temperature. The chain branching reaction R30 plays the most important role on ignition of CH_4 mixtures as it happens also with H_2/air mixtures (Vlachos et al., 1993b). H atoms increase the pool of reactive intermediates with O atoms and OH radicals which attack CH_4 molecules. Increase of the reaction rate of R30 results in considerable promotion of ignition.

Comparison of ignition profiles indicates that there is not a big difference in the profiles between the 6% and 8% CH_4/air mixtures at ignition. The surface mole fractions of H, O, and OH are slightly higher for the 8% mixture. As the equivalence ratio increases, the ignition temperature increases gradually, as indicated in Figure 3c, but the role of the most important reactions on ignition remains almost the same as shown in Figures 6a-6c. Reactions R1 and R30 become more important for fuel richer mixtures whereas reactions R14 and R18 become less important for fuel richer mixtures because O_2 decreases.

In contrast to ignition, the role of kinetics on extinction can vary strongly with equivalence ratio. Extinction of a 6% CH_4/air flame depends strongly on reactions R1, R11, R14, R16, R25, R30, R32, and R34:

$$CO + OH \rightleftharpoons CO_2 + H \quad \text{(R16)}$$

$$O_2 + H + M \rightleftharpoons HO_2 + M^a \quad \text{(R32)}$$

$$O_2 + H + N_2 \rightleftharpoons HO_2 + N_2 \quad \text{(R34)}$$

Reaction R1 consumes H atoms which produce O atoms and OH radicals through the chain branching reaction R30 and increases considerably the extinction temperature. Increase of the rate of reaction R14 produces more HO_2 which leads to increase of the extinction temperature. Reaction R11 produces more H atoms and retards extinction. Reactions R16 and R25 produce H atoms (at the expense of OH radicals or O atoms, respectively) and reduce the extinction temperature. Increase of the rate of reaction R30 increases the amounts of O and OH which retard extinction. Reactions R32-R34, which do not strongly affect ignition of CH_4/air mixtures, consume H atoms to form HO_2. These reactions compete with the chain branching reaction R30 in the consumption of H atoms to form either HO_2 (reactions R32-R34) or O and OH (reaction R30). This is more important at extinction than at ignition, most probably because extinction occurs at quite lower temperatures (~300 K) than ignition where HO_2 is promoted.

The role of kinetics on extinction temperatures of 8% and 12% CH_4/air flames is shown in Figures 6e and 6f. The sen-

sitivity analysis indicates that the thermal decomposition of CH_4 (reaction R1) plays a crucial role on the extinction of these flames. When the preexponential of reaction R1 increases by a factor of 5, the preexponential of the reverse reaction increases by the same amount to keep the equilibrium constant (determined using thermodynamic data). Increase of the preexponential of the reverse recombination reaction, which at low temperatures is the dominant one of two directions, results in considerable reduction of H atoms and hence in an increase of the extinction temperature by ~600 K for 6% and complete extinction for 12% (not shown).

Since extinction temperatures of various composition mixtures can differ substantially, the role of different reactions on extinction is not directly comparable. As an example, reactions R32–R34 are more important for 8% CH_4 in air because they are favored at low temperatures and this mixture has a low extinction temperature. Despite this fact, some important points can be drawn. Reactions R32–R34 produce HO_2 by consuming H atoms and are very important for stoichiometric and fuel rich mixtures. Reaction R1 consumes H atoms to CH_4 and is one of the most responsible reactions for scavenging of H atoms and extinction of flames. Reactions R39 and R42 (termination reactions) become important for fuel rich and stoichiometric to fuel rich mixtures. Reaction R12 (a termination reaction) scavenges H atoms and also becomes important under stoichiometric and fuel rich conditions. Reaction R14 which produces HO_2 and consumes HCO (which can provide H atoms through R11) strongly affects extinction. Reactions R11 and R25 produce H and R30 produces OH and O and can retard remarkably extinction especially of high equivalence ratios. Figures 6d–6f indicate that, as the equivalence ratio increases, some termination reactions become *progressively more important* in promoting extinction.

Reactions R30 and R32–R34 from the submechanism of H_2/air are important reactions also on ignition/extinction of CH_4/air mixtures. Since the pool of H, O, and OH is crucial on ignition/extinction, these reactions would be important in the combustion of other fuels as well. While reactions R32–R34 are important at ignition of H_2 (because it occurs at lower temperatures than CH_4 ignition), they are not essential in the ignition of CH_4/air mixtures. It is anticipated that these reactions would be important for CH_4 or other hydrocarbons at such conditions (equivalence ratio, strain rate) where ignition occurs at lower temperatures. In addition to reactions of the H_2/air mechanism, reactions involving carbon species are also essential in ignition/extinction of CH_4. It might then be expected that details of the ignition depend on the fuel and the conditions.

Role of Strain Rate

The role of strain rate on the bifurcation behavior of CH_4/air mixtures are selected equivalence ratios is shown in Figure 7, where a-d are two parameter bifurcation diagrams in which homogeneous ignition and extinction curves (locus of turning points) are plotted vs. the strain rate α for different compositions of CH_4 in air indicated. These curves are continuations of turning points, such as those shown in Figures 3a and 3b, in a second parameter (strain rate). A constant strain rate line (vertical line) intersects the curves of Figures 7a–7d in two points which are two turning points of a Z-shaped curve such

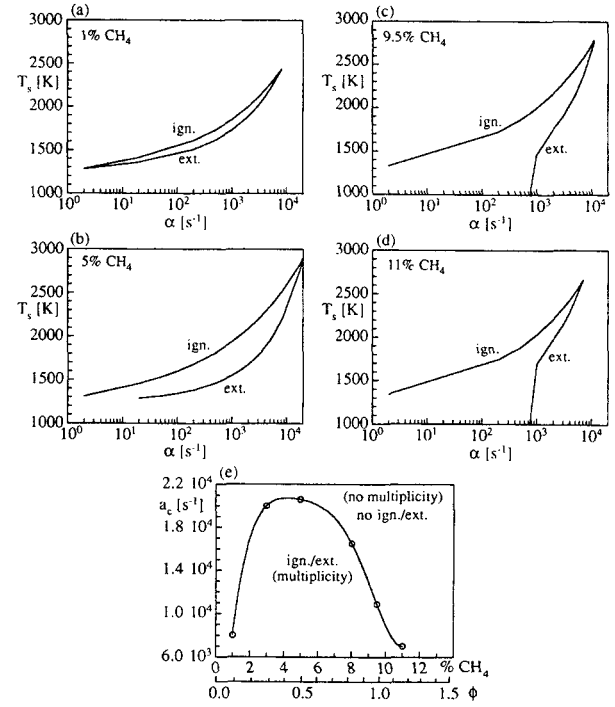

Figure 7. Ignition and extinction temperatures vs. strain rate at different equivalence ratios indicated (a-d) and high critical strain rate vs. equivalence ratio (e).

as those shown in Figures 3a and 3b. As the strain rate (or flow rate) increases, the residence time decreases, and there is not sufficient time for reaction. Thus, increase of the strain rate results in *retardation of ignition* (a higher ignition temperature) and promotion of extinction (a *higher extinction temperature*).

Figures 7a–7d indicate that hysteresis and multiplicity extend over a wide range of strain rates. In contrast to freely propagating flames which can be stabilized for only one velocity (the flame velocity), the stagnation surface supports flames over a wide range of velocities. However, at sufficiently high strain rates ignition and extinction do not occur. The maximum value of strain rate where the ignition and extinction points coincide is called a cusp point (high critical value of strain rate α_c) and corresponds to the maximum strain rate above which no multiplicity exists. The critical strain rate α_c vs. equivalence ratio is shown in Figure 7e. The points in this plot are the locus of critical values of strain rate above which no multiplicity is expected for each equivalence ratio and the solid line is a polynomial fit to the data. The maximum in critical strain rate does not correspond to the stoichiometric point of complete oxidation.

For sufficiently lean mixtures, such as 1% shown in Figure 7a, a minimum strain rate exists below which no hysteresis is observed. This point corresponds to another cusp point (low critical strain rate) caused by small flow rate and energy generation which are not sufficient to cause multiplicity. For larger equivalence ratios, there is a critical strain rate below which extinction of the flame by cold walls is impossible. In these situations, no cusp point is observed at low strain rates (at

least in the physical sense). Figures 7c and 7d are typical examples of such behavior.

Figure 8a shows the distance from the wall of the maximum in the profile of CH_2O (defined here as flame location) vs. the strain rate. As the strain rate increases the flame is pushed towards the wall. At high strain rates the carbon species still peak off the wall (not shown) but the reaction zone is very narrow and adjacent to the wall.

Figures 8b–8f show surface mole fractions (Z-shaped curves) of selected species for 5% CH_4 in air as functions of surface temperature at different strain rates. At low strain rates, complete combustion of CH_4 occurs before it reaches the wall and its surface mole fraction is essentially zero. At high strain rates, the surface mole fraction of CH_4 increases by many orders of magnitude because incomplete reaction occurs due to short residence time. As α increases, ignition and combustion occur at higher surface temperatures so that the chemistry is faster and partly compensates for the reduced residence time. Despite the high surface concentrations of OH and O, CO_2 decreases as α rises because there is not sufficient time for conversion of CO to CO_2. Even though the surface mole fractions of the two oxidizers OH and O are sufficiently high at extinction, extinction occurs at higher temperatures, indicating that low concentration of OH and O is not a necessary condition for extinction, but the residence time and the energy generated are also important factors affecting extinction.

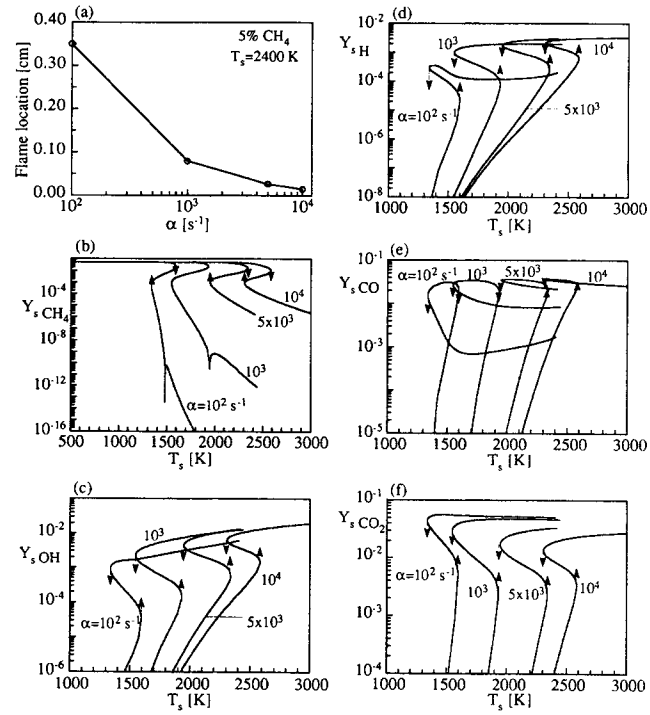

Figure 8. Flame location (peak of CH_2O profile) from the surface vs. strain rate (a).

As α increases the flame is pushed toward the wall. Surface mole fraction of selected species vs. wall temperature at selected strain rates indicated (b–f).

Roles of Intermediate Species and Wall Activity

It has been observed experimentally that catalytic materials frequently increase the temperature for homogeneous ignition (Coward and Guest, 1927; Coward and Greenwald, 1928; Laurendeau, 1982; Griffin and Pfefferle, 1990; Lewis and von Elbe, 1987). It is believed that this is mainly caused by the chemical coupling through reactive intermediates which are common to both homogeneous and heterogeneous phases, and by depletion of reactants in the boundary layer by surface reactions.

Consumption of reactants in rich CH_4/mixtures by a catalyst, that is, depletion of reactants in the boundary layer, leads to richer mixtures which based on Figure 3c would ignite at higher temperatures. On the other hand, depletion of reactants of lean CH_4/mixtures by a catalyst would lead to leaner mixtures which would ignite at lower temperatures. We have actually verified this by showing that an infinitely fast reaction of CH_4 on the wall results in a decrease of the homogeneous ignition temperature of 6% CH_4 in air by ~ 100 K.

The model prediction is however in disagreement with some experimental data for CH_4 where the presence of catalysts result in increased T_{ig}. The increase of T_{ig} or of the ignition time caused by depletion of reactants has also been predicted some time ago for one step global kinetics using asymptotic analysis (Law and Chung, 1983; Linan and Williams, 1981). Trevino (1983), using asymptotic methods, has distinguished between different regimes where catalysts can affect homogeneous combustion. To resolve the discrepancies, we have also used one step global kinetics of Coffee (1985). We found (from constant power surfaces) in agreement with Law and Chung (1983) that the homogeneous ignition exhibits a parabola with a minimum for fuel rich conditions and the change in T_{ig} is very small (only a few degrees). These results (not shown) which mainly capture only the thermal coupling between the surface and the gas phase (but not the chemical interactions between intermediate species) are in complete disagreement with the detailed kinetics used here. Depletion of reactants of lean mixtures in the boundary layer by a catalyst cannot explain the dependence of homogeneous ignition of CH_4 on equivalence ratio. Therefore, we propose that depletion of reactants in the boundary layer does not increase the homogeneous ignition of lean to stoichiometric CH_4/air mixtures, but generation and consumption of intermediates seem to strongly affect homogeneous ignition (see below).

Addition or removal of reactive intermediates can provide information about their role on ignition and extinction, and together with a sensitivity analysis can elucidate the important reaction paths. Addition of radicals in unsteady simulations of CH_4 combustion have been used before (Sloane, 1985; Pfefferle and Churchill, 1983). Addition or removal or reactive intermediates at the surface is particularly interesting because it addresses the fundamental question of how catalysts affect homogeneous reactions. Despite recent laser induced fluorescence experiments, for example, Cattolica and Schefer (1982), Griffin et al. (1989), Williams et al. (1992), and references therein, understanding is poor at the moment of the interplay between homogeneous and heterogeneous reactions.

First the case of an adsorptive surface is considered where an intermediate species is selectively removed (its surface concentration is taken to be zero), whereas the other species do not adsorb on the surface. The results are not meant to describe quantitatively the behavior of real materials because simultaneous adsorption of more than one radical can occur (but

adsorption might not be very fast), and formation of other radicals and stable species at the same conditions followed by desorption can take place. They rather illustrate possible trends that can occur under different conditions. Even though surface sinks or sources lead to a loss of global mass balance, a little error is introduced because of the relatively small concentrations of intermediate species and valuable information about the role of radicals participating in surface reactions is provided.

The effect of radical quenching at walls on homogeneous ignition and extinction of 6% CH_4 in air is shown in Figure 9. Figure 9a shows the change in ignition temperature relative to an inert wall considered above. Consumption of O atoms or OH radicals at the surface results in a moderate increase of the ignition temperature. On the other hand, consumption of CH_3 radicals and H atoms has a very profound effect in increasing the ignition temperature. Figure 9b shows the change in extinction temperature relative to an inert wall. Adsorption of O atoms and OH radicals has a more pronounced effect on extinction than on ignition, H atoms are the most important in determining the extinction temperature, and surface adsorption of CH_3 radicals does not play a role at extinction. Adsorption of the other intermediate species affects only slightly homogeneous ignition and extinction.

Figure 9c shows the surface mole fraction of CH_4 vs. surface temperature for an inert wall and adsorptive walls where one intermediate species (indicated) is heterogeneously consumed. The Z-shaped curve of an inert wall coincides after extinction with that of a wall which adsorbs CH_3. The Z-shaped curves for adsorption of other intermediates show lower reactivity of CH_4 indicating that removal of H, O, and OH results in incomplete combustion of CH_4 and reduced flame stability (higher extinction temperature).

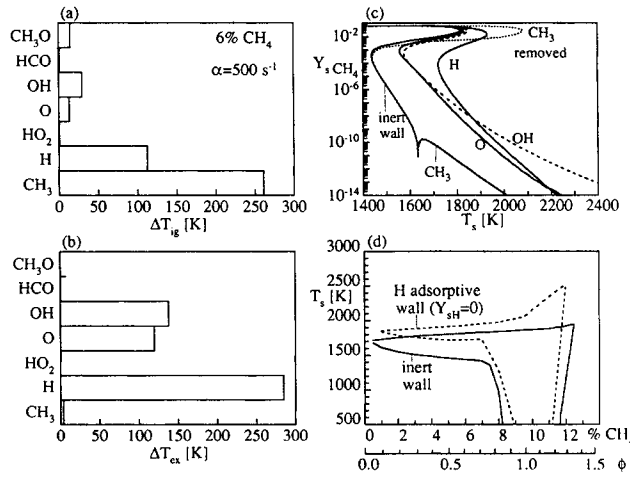

Figure 9. Difference in ignition and extinction temperatures respectively for adsorptive walls (where one species is selectively removed) from those for an inert wall (no adsorption).

(a-b) Surface mole fraction of CH_4 vs. the wall temperature for an inert wall and for adsorptive walls (c). Solid lines show the two parameter bifurcation diagram for an inert wall, and the dashed lines show the corresponding diagram for a wall which selectively removes H atoms (d). Ignition and extinction temperatures can be altered remarkably by surface chemistry, and various species behave differently under different conditions. H atoms become more important under fuel rich conditions. The flammability regime decreases when the surface adsorbs H atoms. 6% CH_4 in air is simulated with $\alpha = 500\ s^{-1}$ (a-d).

Our simulations indicate that removal of certain reactive intermediates by catalysts can result in a remarkable increase of T_{ig} by a few hundred degrees and can explain the increase of homogeneous ignition temperatures of CH_4 and natural gas when oxidized over active materials. Each species can behave in a very different way from other species and under different conditions (compare for example CH_3 at ignition and extinction).

The solid lines in Figure 9d show a two parameter bifurcation diagram for an inert wall (nonadsorptive) and the dashed lines show the same diagram for a H adsorptive wall. Figure 9d indicates that the regime of homogeneous multiplicity is suppressed near adsorptive surfaces and the most pronounced effect of removal of H atoms in increasing the homogeneous ignition temperature occurs for rich mixtures.

Next, the case of a surface which creates intermediates was considered (results not plotted). The behavior can be summarized as follows. Formation of OH and O decreases the ignition temperature, whereas creation of H atoms retards ignition. When the amount of OH radicals or O atoms produced by walls is sufficiently high, no multiplicity occurs, that is, the mixture burns efficiently near the wall (as efficiently as near an inert wall) but without hysteresis. This behavior indicates that the coupling between the heterogeneous and homogeneous processes might not be simply the superposition of the solutions of the individual problems. The homogeneous multiplicity can be wiped out by generation of intermediate species and desorption from the catalyst. This numerical experiment also suggests that it is not only the fractions of O and OH which are important to sustain the homogeneous multiplicity, but the reactions which create them, along with the energy liberated are also crucial.

Ignition and Extinction Mechanisms

As the surface temperature increases along the extinguished branch, the reaction rates of all reactions with positive activation energy and the energy liberated by the exothermic reactions increase. The energy generated increases the temperature which in turn increases the reactions rates due to the Arrhenius kinetics. When the energy formation rate is larger than the energy removal rate (by convection and conduction), an ignition occurs. This is known as thermal runaway event of ignition (Law, 1984). In addition to this feedback temperature mechanism, certain intermediate species and reactions can strongly affect homogeneous ignition.

The recombination reactions R1 and R26 retard ignition. Complete removal of R1, R14, R25, and R26 from the mechanism results in considerable reduction of homogeneous ignition temperature ($\sim$200 K for 6% CH_4 in air). When these reactions are eliminated T_{ig} increases only slightly with composition. Elimination of R1 becomes more important for fuel rich conditions. On the other hand, the chain branching reaction R30, thermal decomposition reactions which produce H atoms, such as R11 and R19, and reactions which convert molecular O_2 to atomic O or OH, such as R18 and R24, promote ignition. As the composition of CH_4 in air increases, the amounts of most intermediate species increase and there is a competition between ignition promoting reactions and ignition

retarding reactions. In the case of hydrogen, the balance favors the promoting reactions, and homogeneous ignition temperatures decrease with ϕ, whereas for CH_4, retarding reactions are favored resulting in an increase of homogeneous ignition temperatures with ϕ. The shortage of H atoms becomes more important for fuel rich conditions (see Figure 9d), where certain termination reactions become fast, resulting in a larger increase of ignition temperature close to the rich flammability limit.

Extinction of flames has been attributed to heat losses either by radiation or conduction and wall quenching, flow nonuniformity such as flame stretch and curvature, and low residence time due to high flow rates (Law, 1984). Since most reactions are activated, at low surface temperatures the reaction rates would decrease, at least near the surface, and the energy generated by the exothermic reactions would decrease. When the energy produced is not sufficient, extinction can occur by wall quenching, a behavior shown for sufficiently fuel lean mixtures in Figure 3c. Chemical quenching through radical recombination and enhancement of termination reactions also could result in extinction.

While the ignition temperature changes gradually with equivalence ratio, the extinction temperature can change dramatically with composition, as shown in Figures 3c and 3d. Some mixtures can be extinguished by a considerable reduction in surface temperature whereas other mixtures cannot be extinguished even though cold walls are quenching the system because many intermediate species are still available far from the wall (in the primary reaction zone) to drive the reactions. Inert walls cannot strongly affect gas-phase reactions through thermal coupling when the flame has moved sufficiently off the wall. In these situations higher strain rates (higher velocities) are required for extinction so that the pool of reactive intermediates becomes sufficiently poor caused by short residence times.

The sensitivity analysis indicates that while termination reactions are not important for fuel lean mixtures, certain termination reactions (indicated in Figure 6e and 6f) become important for mixtures richer than $\sim 7.5\%$ in air for $\alpha = 500$ s^{-1}. As the equivalence ratio increases, the termination reactions become progressively more important and cause chemical quenching (extinction) of fuel rich mixtures. Thus, the dominant mechanism for extinction changes from wall quenching (incomplete reaction) for fuel lean mixtures to chemical quenching (due to termination reactions) for fuel rich conditions. For intermediate compositions, the thermal coupling between the surface and the gas phase can be weak so extinction of the flames cannot occur.

Other Operating Modes of Stagnation Surfaces

Flammability limits for combustion near adiabatic walls have been discussed above (see Figures 3c and 3d). Here, we discuss briefly a constant power surface where the power input to the wall is the control parameter, and the surface temperature is determined by an energy balance at the wall using an appropriate boundary condition (Vlachos et al., 1993). The results of the simulations for this mode can be summarized as follows. Responses of the system are obtained for the surface mole fractions vs. power and for the surface temperature vs. power. Ignition and extinction are observed in the response curves (S- or Z-shaped curves), as for isothermal surfaces, manifested by two turning points. The power requirement for homogeneous ignition is slightly dependent on the equivalence ratio. Extinction cannot be achieved for certain equivalence ratios by cooling the surface, as also happens with isothermal walls.

When the power is the independent variable, the surface temperature at ignition increases very slightly with equivalence ratio. For $\alpha = 200$ s^{-1}, T_{ig} is 1,588 K for 1% CH_4 in air and increases to 1,604 K for 12.5% CH_4 in air, that is, by less than 1%, which is below experimental resolution of usual thermocouples or optical pyrometers. The surface temperature at ignition is comparable with that of an isothermal surface for very lean mixtures, but it can be remarkably lower (by as much as 400 K) for rich mixtures (compare the above values with Figure 3d). Thus, as reported for combustion of H_2 in air (Vlachos et al., 1993b), the operational mode of surfaces can lead to significant differences of bifurcation behavior.

Conclusions

The homogeneous ignition, extinction, and flammability limits of CH_4/air mixtures have been simulated with detailed chemistry including the C1 reaction path with 46 reversible reactions and 16 species, as functions of equivalence ratio and strain rate. The main thrusts of this article can be summarized as follows:

(1) Homogeneous ignition and extinction near isothermal and adiabatic walls occur for a wide range of strain rate (inlet velocity) and equivalence ratio manifested as turning points in Z-shaped curves (or double Z-shaped curves) of surface mole fractions vs. surface temperature. Up to five multiple solutions exist under certain conditions.

(2) The homogeneous ignition temperature increases with equivalence ratio without a maximum around the stoichiometric ratio. The homogeneous extinction temperature decreases gradually with equivalence ratio up to some composition where it drops abruptly and then increases with equivalence ratio for fuel rich mixtures. Mixtures around the stoichiometric ratio cannot be extinguished by cold walls when the strain rate is sufficiently low and are burned more efficiently. Isothermal surfaces extend the flammability limits over insulated walls if energy is provided to the system.

(3) Ignition and extinction cease at sufficiently high strain rates due to short residence times. As the strain rate increases, ignition and extinction temperature rise, and the fuel rich concentration flammability limit decreases.

(4) The dominant extinction mechanism is altered as the composition changes. The extinction of fuel lean and fuel rich mixtures is mainly affected by wall quenching and certain termination reactions respectively. When the flame moves sufficiently off the wall (low strain rates and mixtures around the stoichiometric ratio), the thermal coupling between the surface and the gas phase can be weak and the flame cannot be extinguished by cold walls. The thermal decomposition of CH_4, reaction R1, and the chain branching reaction, R30, are crucial in ignition and extinction of CH_4/air mixtures. It is anticipated that R30 plays a central role in the combustion, ignition, and extinction of many fuels near surfaces.

(5) Surface consumption or generation of reactive intermediates can very strongly affect homogeneous ignition and extinction. OH, O, H, and CH_3 consumption retards homogeneous ignition, whereas surface formation of OH and O

promotes homogeneous ignition. Heterogeneous removal of H, O, and OH plays a profound role in reducing flame stability. The inhibition of homogeneous ignition of CH_4 (or natural gas) in the presence of catalyst is most probably caused by consumption of intermediate species, with H atoms and CH_3 radicals being the most important.

Acknowledgment

This work was supported in part by the Army Research Office contract number DAALO3-89-C-0038 with the University of Minnesota Army High Performance Computing Research Center, by the Minnesota Supercomputer Institute, by DOE under grant number DE-FG02-88ER13878-A02, and by a grant from Shell Petroleum.

Notation

c_p = specific heat of the mixture at constant pressure, cal/g·K
d = nozzle diameter, cm
E = activation energy, cal/mol
f = stream function
k = reaction rate constant; units are moles, cubic centimeters, s
k_o = preexponential; units are moles, cubic centimeters, s
m_g = number of gas-phase species (not counting N_2)
M_j = molecular weight of species j
n_g = number of gas-phase reactions
Pr = Prandtl number
r_i = reaction rate of reaction i, mol/cm^3·s
R = ideal gas constant, cal/mol·K
R_j = consumption or production rate of species j, mol/cm^3·s
Sc_j = Schmidt number of species j
T = absolute temperature, K
v = axial velocity, cm/s
W_j = mass fraction of species j
Y_j = mole fraction of species j
z = axial distance from the wall, cm

Greek letters

α = strain rate, s^{-1}
β = temperature exponent
$-\Delta H_i$ = enthalpy of reaction i, cal/mol·K
η = dimensionless distance
ν_{ij} = stoichiometric coefficient of species j in reaction i
ν = kinematic viscosity, cm^2/s
ρ = gas density, g/cm^3
$\overline{\omega}$ = third body efficiency

Subscripts

o = ambient
s = surface

Literature Cited

Alkidas, A., and P. Durbetaki, "Ignition Characteristics of a Stagnation Point Combustible Mixture," *Combust. Sci. Technol.*, **3**, 187 (1971).

Annamala, K., and M. Sibulkin, "Flame Spread Over Combustible Surfaces for Laminar Flow Systems. Part I: Excess Fuel and Heat Flux," *Combust. Sci. Technol.*, **19**, 167 (1979).

Bond, J., *Sources of Ignition: Flammability Characteristics of Chemicals and Products*, Oxford, Butterworth Heinemann, Boston (1991).

Cattolica, R. J., and R. W. Schefer, "The Effect of Surface Chemistry on the Development of the [OH] in a Combustion Boundary Layer," *Symposium (International) on Combustion/The Combustion Institute*, Vol. 19, p. 311 (1982).

Chin, D.-T., and C.-H. Tsang, "Mass Transfer to an Impinging Jet Electrode," *J. Electrochem. Soc.*, **125**, 1461 (1978).

Coffee, T. P., "On Simplified Reaction Mechanisms by Oxidation of Hydrocarbon Fuels in Flames by C. K. Westbrook and F. T. Dryer," *Combust. Sci. Technol.*, **43**, 333 (1985).

Coward, H. F., and P. G. Guest, "Ignition of Natural Gas-Air Mixtures by Heated Metal Bars," *J. Am. Chem. Soc.*, **49**, 2479 (1927).

Coward, H. F., and H. P. Greenwald, "Propagation of Flame in Mixtures of Natural Gas and Air," Dept. of Commerce, Bureau of Mines, Technical Paper 427 (1928).

Dixon-Lewis, G., C. David, P. H. Gaskell, S. Fukutani, H. Jinno, J. A. Miller, R. J. Kee, M. D. Smooke, N. Peters, E. Effelsberg, J. Warnatz, and F. Behrendt, "Calculation of the Structure and Extinction Limit of a Methane Air Counterflow Diffusion Flame in the Forward Stagnation Region of a Porous Cylinder," *Symposium (International) on Combustion/The Combustion Institute*, Vol. 20, p. 1893 (1984).

Giovangigli, V., and M. D. Smooke, "Extinction of Strained Premixed Laminar Flames with Complex Chemistry," *Combust Sci. Technol.*, **53**, 23 (1987).

Grcar, J. F., R. J. Kee, M. D. Smooke, and J. A. Miller, "A Hybrid Newton/Time-Integration Procedure for the Solution of Steady, Laminar, One-Dimensional, Premixed Flames," *Symposium (International) on Combustion/The Combustion Institute*, Vol. 21, p. 1773 (1986).

Griffin, T. A., L. D. Pfefferle, M. J. Dyer, and D. R. Crosley, "The Ignition of Methane/Ethane Boundary Layer Flows by Heated Catalytic Walls," *Combust. Sci. Technol.*, **65**, 19 (1989).

Griffin, T. A., and L. D. Pfefferle, "Gas Phase and Catalytic Ignition of Methane and Ethane in Air Over Platinum," *AIChE J.*, **36**, 861 (1990).

Kee, R. J., J. A. Miller, G. H. Evans, and G. Dixon-Lewis, "A Computational Model of the Structure and Extinction of Strained, Opposed Flow, Premixed Methane-Air Flames," *Symposium (International) on Combustion/The Combustion Institute*, **22**, p. 1479 (1988).

Kee, R. J., G. Dixon-Lewis, J. Warnatz, M. E. Coltrin, and J. A. Miller, "A FORTRAN Computer Code Package for the Evaluation of Gas-Phase Multicomponent Transport Properties," Sandia National Laboratories Report, SAND86-8246 (1990).

Kee, R. J., F. M. Rupley, and J. A. Miller, "The CHEMKIN Thermodynamic Data Base," Sandia National Laboratories Report, SAND87-8215B (1991).

Kee, R. J., E. Meeks, J. A. Miller, T. Takeno, M. Nishioka, and R. W. Dibble, "On the Practical Exploitation of Strained Laminar Premixed Flames," submitted (1993).

Laurendeau, N. M., "Thermal Ignition of Methane Air Mixtures by Hot Surfaces: A Critical Examination," *Combust. Flame*, **46**, 29 (1982).

Law, C. K., "On the Stagnation-Point Ignition of a Premixed Combustible," *Int. J. Heat Mass Transfer*, **21**, 1363 (1978).

Law, C. K., and S. H. Chung, "Thermal and Catalytic Inhibition of Ignition Through Reactant Depletion," *Combust. Sci. Technol.*, **32**, 307 (1983).

Law, C. K., "Heat and Mass Transfer in Combustion: Fundamental Concepts and Analytical Techniques," *Prog. Energy Combust. Sci.*, **10**, 295 (1984).

Lewis, B., and G. von Elbe, *Combustion, Flames and Explosions of Gases*, Academic Press, Orlando (1987).

Linan, A., and F. A. Williams, "Note on Ignition by a Hot Catalytic Surface," *SIAM J. Appl. Math.*, **40**, 261 (1981).

Miller, J. A., R. J. Kee, and C. K. Westbrook, "Chemical Kinetics and Combustion Modeling," *Annu. Rev. Phys. Chem.*, **41**, 345 (1990).

Pfefferle, L. D., and S. W. Churchill, "A Computer Study of the Constant Pressure Auto-Ignition of Mixtures of Ethane, Methane, Carbon Monoxide and Hydrogen in Air," *ASME 83-WA/HT-67*, 1 (1983).

Rogg, B., "Response and Flamelet Structure of Stretched Premixed Methane Air Flames," *Combust. Flame*, **73**, 45 (1988).

Rogg, B., "Numerical Modeling and Computation of Reactive Stagnation-Point Flows," in: *Computers and Experiments in Fluid Flow*, G. M. Carlomagno and C. A. Brebbia, eds., Springer, Berlin, p. 75 (1989).

Sharma, O. P., and W. A. Sirignano, "Ignition of Stagnation Point Flow by a Hot Body," *Combust. Sci. Technol.*, **1**, 95 (1969).

Sloane, T. M., "The Effect of Selective Energy Deposition on the Homogeneous Ignition of Methane and Its Implications for Flame Initiation and Combustion Enhancement," *Combust. Sci. Technol.*, **42**, 131 (1985).

Smith, H. W., R. A. Schmitz, and R. G. Ladd, "Combustion of a Premixed System in Stagnation Flow—I. Theoretical," *Combust. Sci. Technol.*, **4**, 131 (1971).

Song, X., L. D. Schmidt, and R. Aris, "The Ignition Criteria for Stagnation-Point Flow: Semenov-Frank-Kamenetski or van't Hoff," *Combust Sci. Technol.*, **75**, 311 (1991a).

Song, X., W. R. Williams, L. D. Schmidt, and R. Aris, "Bifurcation Behavior in Homogeneous-Heterogeneous Combustion: II. Computations for Stagnation-Point Flow," *Combust. Flame*, **84**, 292 (1991b).

Spalding, D. B., and P. L. Stephenson, "Laminar Flame Propagation in Hydrogen and Bromine Mixtures," *Proc. Roy. Soc. Lond. A*, **324**, 315 (1971).

Trevino, C., "Gas-Phase Ignition of Premixed Fuel by Catalytic Bodies in Stagnation Flow," *Combust. Sci. Technol.*, **30**, 213 (1983).

Vlachos, D. G., L. D. Schmidt, and A. Aris, "Products in Methane Combustion Near Surfaces," *AIChE J.*, **40**(6), 1018 (1994).

Vlachos, D. G., L. D. Schmidt, and R. Aris, "Ignition and Extinction of Flames Near Surfaces: Combustion of H_2 in Air," *Combust. Flame*, **95**, 313 (1993).

Warnatz, J., "Rate Coefficients in the C/H/O System," *Combustion Chemistry*, W. C. Gardiner, Jr., ed., Springer, Berlin, p. 197 (1984).

Westbrook, C. K., and F. L. Dryer, "Chemical Kinetic Modeling of Hydrocarbon Combustion," *Prog. Energy Combust. Sci.*, **10**, 1 (1984).

Williams, W. R., C. M. Marks, and L. D. Schmidt, "Steps in the Reaction $H_2+O_2 \rightleftharpoons H_2O$ on Pt: OH Desorption at High Temperatures," *J. Phys. Chem.*, **96**, 5922 (1992).

Manuscript received May 3, 1993, and revision received Sept. 10, 1993.